Regular Article

Optimization of the Adsorption of Pb(II) and Zn(II) onto the EDTA-Modified MnO₂/Chitosan/Fe₃O₄ Nanocomposite from an Aqueous Solution Using RSM According to the CCD Method

A. Panahandeh [1], A. Parvareh [2, 3], M. Keshavarz Moraveji [4]*

[1] *Department of Chemical Engineering, Borujerd Branch, Islamic Azad University, Borujerd, Iran*
[2] *Faculty of Petroleum and Chemical Engineering, Razi University, P. O. Box: 6714967346, Kermanshah, Iran*
[3] *CFD Research Group, Advanced Chemical Engineering Research Center, Faculty of Petroleum and Chemical Engineering, Razi University, P. O. Box: 6714967346, Kermanshah, Iran*
[4] *Department of Chemical Engineering, Amirkabir University of Technology (Tehran Polytechnic), Tehran, Iran*

ARTICLE INFO

ABSTRACT

The central composite design (CCD) was employed to investigate the adsorption of Pb(II) and Zn(II) metal ions as well as methylene blue (MB) as an aromatic anion by a new EDTA/MnO₂/CS/Fe₃O₄ synthesized nanocomposite. The effect of possible affective factors including the contaminant concentration (20-200 mg/L), pH (2-8), adsorbent content (0.1-0.9 g/L), and contact time (10-110 min) on the adsorption of the metal ions using response surface methodology (RSM) were studied. The highest removal percentages predicted by the model were 100.776 % and 87.069 %, respectively, for the removal of Pb(II) and Zn(II), that the value of more than 100 % in the case of Pb(II) was due to the model's error. The effect of the simultaneous presence of methyl blue (MB) and the metal ions in the aqueous solution on the adsorption rate of each metal ion was investigated. The study of the adsorption isotherms in the single-component adsorption showed the dominance of Langmuir isotherm over the adsorption process of each pollutant ($R^2 > 0.99$). The maximum adsorption capacities according to the Langmuir model were 310.4 and 136 mg/g for lead and zinc ions, respectively, and 421.1 mg/g for methyl blue. The results showed that the studied nanocomposite still had high efficiency after five consecutive adsorption-desorption cycles.

1. Introduction

Heavy metals such as lead, nickel, copper,

*Corresponding author: arsalanparvareh@yahoo.com, a.parvareh@razi.ac.ir (A. Parvareh)

mercury, zinc, cadmium, and iron with a relative atomic mass of 63.5 to 200.6 and a density of more than 6 g/cm^3 are the most common contaminants that cause serious damages to the environment [1-4]. Lead, which is one of the most widely used base metals in industry, is a heavy and bluish-gray metal with an atomic number of 82 and a melting point of 327 °C. According to the US Environmental Protection Agency standard (EPA standard, 2018), although there is no safe level for lead in drinking water, its activity level is 0.015 mg/L. Nevertheless, lead is still used as a pigment in ceramic glazes, plumbing fittings, lead- acid batteries, decorative objects [1, 3, 5, 6].

Zinc is another widely used metal in the industry. The permissible content in drinking water is 5 mg/L. Large amounts of zinc metal ions in water are very toxic to plants, trees, aquatics, and invertebrates [7, 8].

Some of methods for removing these contaminants from effluents and sewage and the entire environmental cycle include the ion exchange, membrane filtration, flotation, biological removal, electro-deionization, chemical precipitation, adsorption process, and several other methods [9-11]. The adsorption process has received more attention from researchers owing to its easy operation, wide availability, high performance, and economic efficiency [12, 13]. Chitosan is a hydrophilic and cationic polymer obtained by the removal of chitin acetyl groups in the alkaline media [2, 12, 14] which have a very high potential to remove contaminants such as metal ions, radioactive materials, various pigments, phenols, and also various anions from water. There are several sources for extracting the chitosan biopolymer, such as crab skins, shrimp, insect cuticles, and the cell wall of some fungi and algae [15, 16].

Although, chitosan has high efficiency in adsorbing heavy metals due to the presence of hydroxyl and amine groups in its structure, some of the negative properties of this biopolymer such as swelling in water systems, instability in acidic solutions, and poor mechanical properties have restricted its applications [1, 2]. Therefore, to strengthen its structure, metal oxides such as magnetite, cerium oxide, zinc oxide, and many other metal oxides are used. Also, to modify the surface and strengthen the physical properties of chitosan, it's cross-linking with some functional chemicals such as epichlorohydrin, triphosphate, glutaraldehyde, and EDTA is used [17]. In a study, the surface of α-MnO_2 nanorods was activated with aminopropyl triethoxylan. Then they used it as filler for Chitosan nanocomposite and finally cross-linked the resulting nanocomposite with glutaraldehyde. Based on the gravimetric analysis, the content of aminopropyl triethoxylan in manganese dioxide was 20 % by weight. The results showed that the crosslinking has increased the thermal stability of the chitosan nanocomposite [16]. Among the mentioned materials for modifying the surface and strengthening the physical properties of chitosan, EDTA, as a strong chelating agent, forms stable chelates with metal ions, thus increases the adsorption power [2, 18].

In our previous study [1], a new EDTA/MnO_2/Chitosan/Fe_3O_4 nanocomposite was synthesized and modified using EDTA. The XRD, SEM, TEM, FTIR, and EDAX analyzes were used to evaluate the properties and characteristics of the synthesized nanocomposites. The synthesized nanocomposite was used for the adsorption of Pb(II) and Zn(II). Different isotherm models

for single-component adsorption (including Langmuir, Freundlich, Temkin , and Dubinin-Radushkovich model) as well as Simultaneous adsorption models (Non-modified Langmuir model, Modified Langmuir isotherm model, Extended Freundlich isotherm model, Langmuir-Freundlich binary adsorption isotherm), were investigated and their related parameters were obtained. Furthermore, a kinetics and thermodynamic study of adsorption were done The influence of the initial pH, as well as the contact time on the zinc(II) and lead(II) adsorption, was studied [1].

In the present study, the removal of divalent lead and zinc heavy metals by a synthesized nanocomposite (EDTA/MnO$_2$/Chitosan/Fe$_3$O$_4$) was investigated. The impact of four effective process factors (including the initial concentration of metal ions, adsorbent dose, pH, and contact time) on the adsorption process was studied using the central composite design (CCD) of RSM. The optimal adsorption conditions and the highest lead and zinc metal ions removal were predicted under these conditions and compared with the actual experimental values. Then, the impact of the simultaneous presence of the methyl blue (MB) as an aromatic anion and the metal ions in an aqueous solution on the adsorption rate of each pollutant was investigated. Finally, the dominant adsorption isotherms in single-component and binary-component systems were determined.

2. Experimental
2.1. Experiment method
Five levels for the initial concentrations of the metal ion (mg/L), pH, adsorbent dose, and contact time were considered as the affecting parameters in the adsorption process of metal

ions. Experiments were performed in 50 ml Erlenmeyer flasks containing 20 mL of Pb(II) or Zn(II) solutions with different concentrations of metal ions (according to the design of experiments). Also, different values of EDTA/γ-MnO$_2$/CS/Fe$_3$O$_4$ nano sorbent were used in each experiment. The contents of the flasks were agitated at 150 rpm using a shaker for the specified time for each experiment. The pH of the solution was measured using a Metrohm 692 pH meter (Herisau, Switzerland) and adjusted using 0.1 M solutions of caustic and nitric acid. The concentration of each contaminant was determined using an atomic absorption spectrometer at the end of each experiment, and the adsorption rate of each contaminant by nano sorbent at the contact time of t was obtained according to the below relation [19].

The adsorption capacity (or adsorption rate) at the time of t (q_t) and equilibrium adsorption capacity (q_e) were calculated according to Eqs. (1) and (2), respectively :

$$q_t = \frac{V(C_0 - C_t)}{m} \tag{1}$$

where C_0 and C_t are the contaminant concentrations in terms of mg/L at the beginning of the experiment (t=0) and at the contact time of t, V denotes the volume of the solution in mL and m represents the nano sorbent mass in terms of g, respectively. The equilibrium adsorption rate of each contaminant was obtained from the below equation [19].

$$q_e = \frac{V(C_0 - C_e)}{m} \tag{2}$$

where C_e is the concentration of the contaminant (mg/L) at the equilibrium state. The following equation was applied for the computation of the removal percentage of

each metal ion [20]:

$$\% \text{ Removal} = \frac{C_0 - C_t}{C_0} * 100 = \frac{q_t * m/V}{C_0} * 100 \quad (3)$$

2.2. Experiment design

The central composite design (CCD) method is based on the second-order model which plays a very important role in the RSM, because in addition to the ability to display different modes of curve functions, estimating the parameters of this model is also very easy [21-23]. In this method, the levels related to independent variables are coded to equalize the ranges of these variables and have easier regression analyses. Therefore, each factor is examined at five levels of $+\alpha$, $+1$, 0, -1, and $-\alpha$ in which the selection of α is optional and can be valued smaller than one. Finally, an experimental model for predicting the responses as a function of factors is obtained using the following polynomial equation [24, 25]:

$$Y = \beta_0 + \sum_{i=1}^{k} \beta_i x_i + \sum_{i=1}^{k} \beta_{ii} x_i^2 +$$

$$\sum_{i=1}^{k} \sum_{j=1}^{k} \beta_{ij} x_i x_j + \varepsilon \quad (4)$$

where Y represents the expected value of the response variable, k is the number of factors, x_i is the coded value of the independent variable i, β_0 is a constant value, β_i is the coefficient of the linear effect of factor i, β_{ij} is the interaction of coefficient or interaction of two factors i and j and β_{ii} is the second-order effect coefficient of factor i.

In this study, the effect of four effective and important factors of the metal ion concentration (mg/L), adsorbent dose (g/L), pH, and contact time (min) on the adsorption of Pb(II) and Zn(II) metal ions by nano sorbent were evaluated. Table 1 shows the main and coded levels of the mentioned factors.

Table 1

The levels of the factors and related codes for the experimental design by RSM, CCD method.

Operating factors	Symbol	Main levels and related codes				
		-1	-0.5	0	+0.5	+1
pH	X_1	2	3.5	5	6.5	8
Metal ion initial concentration (mg/L)	X_2	20	65	110	155	200
Adsorbent Dose (g/L)	X_3	0.1	0.3	0.5	0.7	0.9
Contact Time (min)	X_4	10	35	60	85	110

According to this table, the value of α is less than one and is selected equal to 0.5. This causes more experiments to be performed at the boundary values of the factors and the sensitivity of the response to changes in the variables to be clearer. Therefore, a better analysis is performed for the results.

The design Expert software was used to

design the experiments. This software uses 6 central points for four input factors on five different surfaces. In other words, the number of repetitions of the experiment, when all the factors are at their central value, is equal to 6 runs. Taking into account the number of 16 basic experiments based on the factorial design and 8 axial points, the total number of

experiments is equal to 30.

3. Results and discussion

3.1. Experimental design and the determination of the optimal adsorption conditions of Pb(II) and Zn(II) by the synthesized nano sorbent

To study and evaluate the effect of pH, metal ion concentration, adsorbent dose, and contact time factors on the adsorption capacity of EDTA/γ-MnO$_2$/CS/Fe$_3$O$_4$ nanocomposite in the adsorption of lead and zinc metal ions, and also to investigate the interaction of these factors, adsorption experiments were designed and implemented. The results of the adsorption of metal ions based on the CCD experimental design are shown in Table 2.

Table 2
Experimental design matrix and the results of the performed experiments.

Experiment	X$_1$: pH	X$_2$: Metal ion initial concentration (mg/lit)	X$_3$: Adsorbent dosage (g/lit)	X$_4$: Contact time (min)	Pb(II) Removal (%)	Pb(II) Adsorbing capacity (mg/g)	Zn(II) Removal (%)	Zn(II) Adsorbing capacity (mg/g)
1	2	20	0.1	10	19.40	38.80	11.92	23.84
2	8	20	0.1	10	32.74	65.48	24.13	48.26
3	2	200	0.1	10	1.48	29.60	4.91	98.20
4	8	200	0.1	10	13.62	272.40	6.83	136.60
5	2	20	0.9	10	23.00	5.11	19.22	4.27
6	8	20	0.9	10	46.49	10.33	39.47	8.77
7	2	200	0.9	10	9.00	20.00	8.74	19.42
8	8	200	0.9	10	21.36	47.47	15.08	33.51
9	2	20	0.1	110	28.12	56.24	21.28	42.56
10	8	20	0.1	110	45.87	91.74	39.00	78.00
11	2	200	0.1	110	12.73	254.60	6.17	123.40
12	8	200	0.1	110	13.55	271.00	6.46	129.20
13	2	20	0.9	110	51.60	11.47	42.60	9.47
14	8	20	0.9	110	87.49	19.44	80.61	17.91
15	2	200	0.9	110	27.31	60.69	20.66	45.91
16	8	200	0.9	110	50.11	111.36	42.23	93.84
17	3.5	110	0.5	60	49.61	109.14	41.85	92.07
18	6.5	110	0.5	60	63.26	139.17	41.13	90.49
19	5	65	0.5	60	67.44	87.67	55.67	72.37
20	5	155	0.5	60	63.19	195.89	43.98	136.34
21	5	110	0.3	60	57.57	211.09	39.42	144.54
22	5	110	0.7	60	69.04	108.49	55.60	87.37
23	5	110	0.5	35	54.20	119.24	41.85	92.07
24	5	110	0.5	85	70.40	154.88	54.20	119.24

25	5	110	0.5	60	67.64	148.81	48.23	106.11
26	5	110	0.5	60	64.26	141.37	53.35	117.37
27	5	110	0.5	60	61.04	134.29	52.14	114.71
28	5	110	0.5	60	67.02	147.44	50.54	111.19
29	5	110	0.5	60	64.61	142.14	53.20	117.04
30	5	110	0.5	60	63.00	138.60	48.99	107.78

Applying the experimental results, the Quadratic model with the R^2 values of 0.9876 and 0.9840 was proposed for Pb(II) and Zn(II) adsorption respectively. Table 3 shows the results for the analysis of variance of the quadratic model for the adsorption of the desired metal ions. In general, the larger F-value and the smaller P-value for a term of the model shows that the mentioned term in the model has been more important. P-value < 0.05 indicates the significance, 0.05 < P-value < 0.1 indicates the quasi-significance, and P-value > 0.1 indicates the insignificance of a parameter [26, 27]. As observed, the F-values of the two models for lead and zinc ions are 85.12 and 65.07, respectively, and the P-values of both models are less than 0.0001 (i.e. the probability that the F-values for each model which are due to noise are less than 0.01 %). The values of F and P indicate that the proposed quadratic models are well compatible with the experimental results for both ions. Another important parameter, which is used to analyze the model, is the Lack of Fit (LOF) test. LOF is a comparison of residual error and pure error, and in here, its insignificance is desirable. It can be said that a small value of LOF related to F-value (compared to pure error) and a probability of more than 10 % (LOF P-value > 0.1) are necessary for the accurate prediction of the response. The F-values of the LOF of the lead and zinc adsorption models are 2.66 and 3.24, and the P-values of the same are 0.1454 and 0.1034, respectively, which indicate relatively good compatibility and fitting of the model to the results. But among the different terms shown in Table 3, terms X_2X_3, X_2^2, X_3^2, and X_4^2 are insignificant for the models related to both ions and also the X_1X_4 term for the model related to Pb(II) ion. The elimination of the insignificant terms usually helps to improve the model and leads to more accurate results [28].

Table 3

Analysis of variance of the quadratic model for the adsorption of lead and zinc ions by the nano sorbent (before modifying the model).

Source	Pb(II)					Zn(II)				
	df	Mean Sum of Square	F-value	P-value		df	Mean Sum of Square	F-value	P-value	
Model	14	1094.09	85.12	< 0.0001	Sign.	14	770.56	65.70	< 0.0001	Sign.
X_1	1	1281.89	99.73	< 0.0001		1	842.99	71.88	< 0.0001	
X_2	1	2135.05	166.10	< 0.0001		1	1813.57	154.64	< 0.0001	
X_3	1	1448.18	112.66	< 0.0001		1	1474.63	125.74	< 0.0001	

	df	Mean Sum of Square	F-value	P-value		df	Mean Sum of Square	F-value	P-value	
X_4	1	1508.66	117.37	< 0.0001		1	1102.60	94.01	< 0.0001	
X_1X_2	1	112.07	8.72	0.0099		1	210.85	17.98	0.0007	
X_1X_3	1	159.27	12.39	0.0031		1	182.49	15.56	0.0013	
X_1X_4	1	15.87	1.23	0.2840		1	84.92	7.24	0.0168	
X_2X_3	1	16.11	1.25	0.2805		1	33.75	2.88	0.1105	
X_2X_4	1	68.86	5.36	0.0352		1	148.68	12.68	0.0028	
X_3X_4	1	437.02	34.00	< 0.0001		1	384.85	32.81	< 0.0001	
X_1^2	1	150.94	11.74	0.0037		1	123.12	10.50	0.0055	
X_2^2	1	4.87	0.3792	0.5472		1	6.29	0.5359	0.4754	
X_3^2	1	1.17	0.0910	0.7671		1	1.61	0.1370	0.7164	
X_4^2	1	7.37	0.5736	0.4606		1	0.1921	0.0164	0.8999	
Residual	15	12.85				15	11.73			
Lack of Fit	10	16.24	2.66	0.1454	Not sign.	10	15.24	3.24	0.1034	Not sign.
Pure Error	5	6.09				5	4.71			
Cor Total	29					29				

After modifying the model and eliminating the insignificant terms (P-value > 0.1), modified models were obtained without any insignificant terms. It is worth noting that modifying the model and eliminating an insignificant term may make the same term significant or quasi-significant. For example, in the present study, the X_2X_3 term with a P-value greater than 0.1, as shown in Table 4, its P-value has decreased to 0.0847 and therefore has become quasi-significant.

According to other information presented in Table 4, the modified model has higher compatibility and validity for predicting results. For example, the LOF F-values for the two models related to lead(II) and zinc(II), have decreased to 2.26 and 2.60, respectively, which is not significant compared to the pure error of the models (30.46 and 23.54). Also, the LOF P-values of the two models have increased to 0.1883 for Pb(II) and 0.1497 for Zn(II).

Table 4
Analysis of variance of the quadratic model for the adsorption of lead and zinc ions by the nano sorbent (after modifying the model and deleting insignificant terms P-value > 0.1).

Source		Pb(II)					Zn(II)			
	df	Mean Sum of Square	F-value	P-value		df	Mean Sum of Square	F-value	P-value	
Model	9	1697.04	143.37	< 0.0001	Sign.	11	980.12	96.69	< 0.0001	Sign.
X_1	1	1281.89	108.30	< 0.0001		1	842.99	83.16	< 0.0001	
X_2	1	2135.05	180.37	< 0.0001		1	1813.57	178.91	< 0.0001	

X_3	1	1448.18	122.35	< 0.0001		1	1474.63	145.47	< 0.0001	
X_4	1	1508.66	127.45	< 0.0001		1	1102.60	108.77	< 0.0001	
X_1X_2	1	112.07	9.47	0.0059		1	210.85	20.80	0.0002	
X_1X_3	1	159.27	13.46	0.0015		1	182.49	18.00	0.0005	
X_1X_4						1	84.92	8.38	0.0097	
X_2X_3						1	33.75	3.33	0.0847	
X_2X_4	1	68.86	5.82	0.0256		1	148.68	14.67	0.0012	
X_3X_4	1	437.02	36.92	< 0.0001		1	384.85	37.96	< 0.0001	
X_1^2	1	8122.36	686.19	< 0.0001		1	4501.96	444.11	< 0.0001	
Residual	20	11.84				18	10.14			
Lack of Fit	15	13.75	2.26	0.1883	Not sign.	13	12.23	2.60	0.1497	Not sign.
Pure Error	5	6.09				5	4.71			
Cor Total	29					29				

Improved quadratic models for the adsorption of Pb(II) and Zn(II) ions in a single component system have been obtained as:

% Pb(II) Removal = $64.21 + 8.81 X_1 - 11.38 X_2 + 9.37 X_3 + 9.56 X_4 - 2.65 X_1X_2 + 3.16 X_1X_3 - 2.07 X_2X_4 + 5.23 X_3X_4 - 33.94 X_1^2$ (5)

% Zn(II) Removal = $49.55 + 7.15 X_1 - 10.48 X_2 + 9.45 X_3 + 8.17 X_4 - 3.63 X_1X_2 + 3.38 X_1X_3 + 2.30 X_1X_4 - 1.45 X_2X_3 - 3.05 X_2X_4 + 4.90 X_3X_4 - 25.27 X_1^2$ (6)

According to the coefficients of these equations (presented in terms of coded factors), the effect of parameter X_2 (the initial concentration of the metal ion) on the response in models is greater than the effect of other parameters, and this effect is negative, i.e. the removal decreases by increasing the initial concentration of metal ions. It can also be said that pH and contact time changes on Pb(II) are more effective than thoes on Zn(II). The opposite of this point is established poorly for the adsorbent dose.

The two modified models have R^2 values of 0.9847 and 0.9834 for Pb(II) and Zn(II) respectively (Table 5), which indicate good consistency between the model and experimental results.

Table 5
Determination coefficients, standard deviation, and coefficient of the variation of the quadratic models obtained for the adsorption of Pb(II) and Zn(II) in the single-component system.

	Pb(II)	**Zn(II)**		**Pb(II)**	**Zn(II)**
Std. Dev.	3.44	3.18	R^2	0.9847	0.9834
Mean	45.54	35.65	Adjusted R^2	0.9779	0.9732
C.V. %	7.56	8.93	Predicted R^2	0.9492	0.9314
			Adeq precision	39.3888	37.1696

The small difference between the adjusted R^2 and predicted R^2 (difference less than 0.2) indicates the logical compatibility of these two coefficients of determination. An important parameter of Adeq Precision is the signal-to-noise ratio, which indicates the difference between the predicted response value and the average predicted error value; a value greater than 4 indicates the appropriate detection of the model. According to Table 5, the values of this parameter are greater than 4 for both models.

The maximum Pb(II) removal has been predicted to be 100.776 % (greater than 100 is due to the model's error). The optimal conditions for this response are the pH of 5.601, initial concentration of 34.379 mg/L of Pb(II), adsorbent dose of 0.892 g/L and contact time of 109.776 min. The experiment performed under the above laboratory conditions resulted in the 99.37 % removal of Pb(II) ions, which had only a 1.41 % diviation from the value estimated by the model and indicated the accuracy of the proposed model. The maximum value predicted by the model for the removal of Zn(II) from the aqueous solution by the studied nano sorbent was 87.06 %, which was obtained under the optimal conditions of the pH value equal to 5.911, initial concentration of 285.29 mg/L of Pb(II), adsorbent dose of 0.877 g/L and contact time of 109.923 min. The actual response obtained under the mentioned optimal conditions was equal to 85.21 which was different from the predicted value by only 2.2 % and showed that the obtained model had good accuracy for predicting the response.

The 3D diagrams of response surfaces, corresponding to the unprompted models, can be used to evaluate the effect of interactions of the process variables on the response and compare them with each other. Figure 1 presents the 3D diagrams of the response surfaces related to the interaction of experimental variables in the adsorption of lead bivalent ions (the 3 D diagrams related to the adsorption of zinc on the nanocomposite has a similar trend to the adsorption of lead and have not been presented here). Using these diagrams, it is possible to study the simultaneous effect of two factors on the response and determine the areas where the maximum pollutant removal occurs.
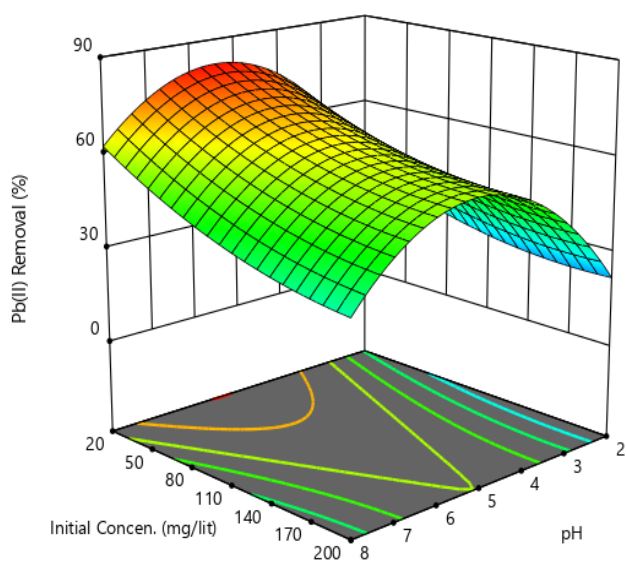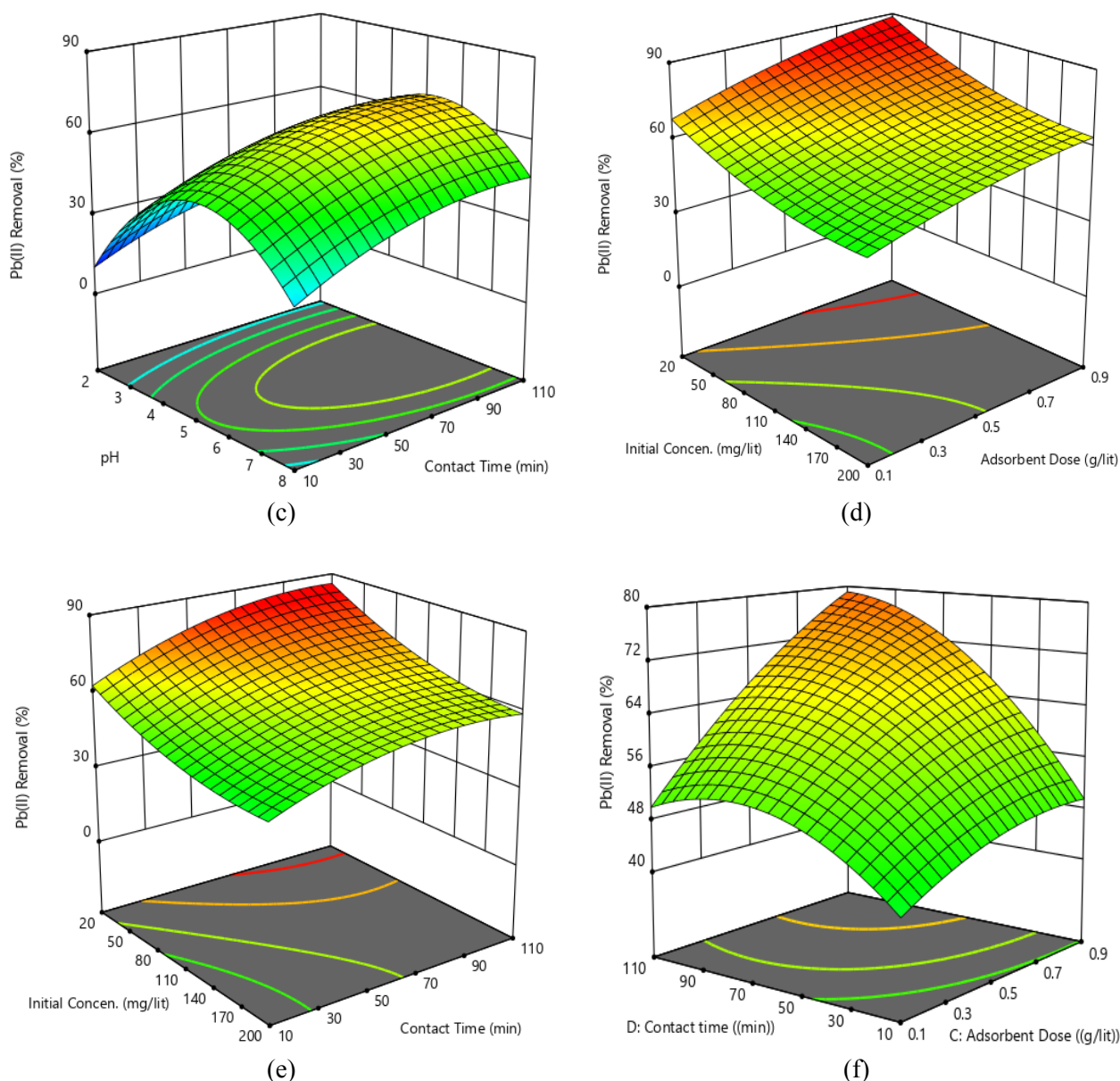

(a)
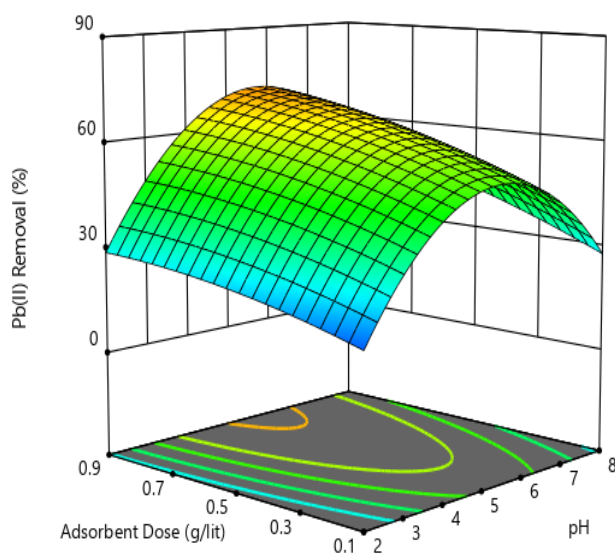
(b)

Figure 1. 3D diagrams of the effect of interactions on the Pb(II) removal by the EDTA/γ-MnO$_2$/CS/Fe$_3$O$_4$ nanocomposite from the aqueous solution, (a) pH, the Pb(II) initial concentration, (b) pH, the adsorbent dose, (c) pH, the contact time, (d) the Pb(II) initial concentration, adsorbent dose, (e) the Pb(II) initial concentration, contact time, (f) the adsorbent dose, contact time.

Generally, as the initial concentration of the pollutant ions increases, the removal decreases due to the saturation of the active sites of the adsorbent. In 3D diagrams that show the interaction of pH with the initial concentration (C$_0$) of the lead ion (Figure 1a), it can be seen that the removal of each metal cation increases by increasing pH in the acidic environment. This incremental trend continues up to the pH values in the range of

5 to 6, but the removal decreases gradually at the pH values above this range.

The increasing trend of the removal from low pH values to high pH values is related to the nano sorbent pH$_{PZC}$ (4.6). As long as the pH of the aqueous solution has this value, the nano sorbent surface has a neutral charge. At the pH values of below 4.6, the nanocomposite surface has a positive charge due to the accumulation of hydrogen cations,

and the protonation of some functional groups belonging to chitosan and EDTA and their conversion to positive ions (such as NH_3^+) are much easier. Therefore, at the pH values of lower than pH_{PZC}, the adsorption rate and therefore the removal will have their lowest values owing to the electrostatic repulsion of the surface and also the competition between the lead (or zinc) metal ion and other cations. At the pH values of above pH_{PZC}, negative ions such as OH^- and COO^- and more generally $-RO^-$ increase at the nanocomposite surface causing the surface to become negatively charged. Therefore, the adsorption of metal cations due to the electrostatic attraction and less competition is easier.

At the pH values of above 6, hydroxyl complexes and metal hydroxide deposits are formed, which are not desirable for the adsorption process and reduce the adsorption rate [29, 30]. In the 3D diagrams showing the interaction of pH with the adsorbent dose, in addition to the above points, it is observed that at alkaline pH values compared to acidic ones, increasing the adsorbent dose has a greater effect on the removal. This can be attributed to the surface charge of the nanocomposite at acidic pH values.

In all diagrams related to the simultaneous effects of the absorbent dose and another factor on the response variable it was observed that in low doses, by increasing the adsorbent dose, the removal also increases. But at higher doses, this increasing trend has stopped or changed to a decreasing trend. This is because increasing the adsorbent dose increases the active sites and functional groups at low doses, so the removal also increases. However, at high doses, the removal is not increased much due to the reduced probability of the contact of adsorbate ions and adsorbent nanoparticles

[26]. In Figure 1f, it is observed that at high doses of the nano sorbent, by increasing the contact time, the removal also increases with a great slope, until after a sufficient time and the saturation of active sites, this slope decreases and eventually becomes almost zero. But, due to the rapid saturation of active sites at low doses, the increasing trend of the removal does not take much time, and after 70 min, the slope of the increasing trend of the removal becomes zero, and then metal ions may be repelled due to the weakening of van der Waals bonds. It should be noted that the behavior of the dependent variables of the adsorption capacity and the removal in relation to the factors of the initial concentration and the adsorbent dose are opposite to each other and concerning the factors of pH (in the acidic environment) and the contact time are similar.

3.2. Comparison of the effect of the initial pH of the solution on the adsorption of MB and metal ions

There are always several contaminants from one or more different organic and inorganic groups in the industrial effluents, and the presence of only one single pollutant in industrial effluents is rare. Therefore, in the present study, the adsorption of metal ions (as cations) and methylene blue (MB) (as an aromatic anion) were considered. To evaluate the effect of the initial pH of the solution on the adsorption of MB by nanocomposites and compare it with the results obtained for the adsorption of metal ions, the MB adsorption was performed at the pH values in the range of 2 to 10 (the adsorbent dose: 0.5 g/L, the initial concentration of MB: 200 mg/L, temperature: 25 °C). According to the results shown in Figure 2, at acidic pH values, the maximum adsorption capacity is obtained for

the removal of MB (unlike metal cations). The decreasing trend of the adsorption begins at the pH values higher than $pH_{PZC}=4.6$ and reaches its lowest value at the pH=10.
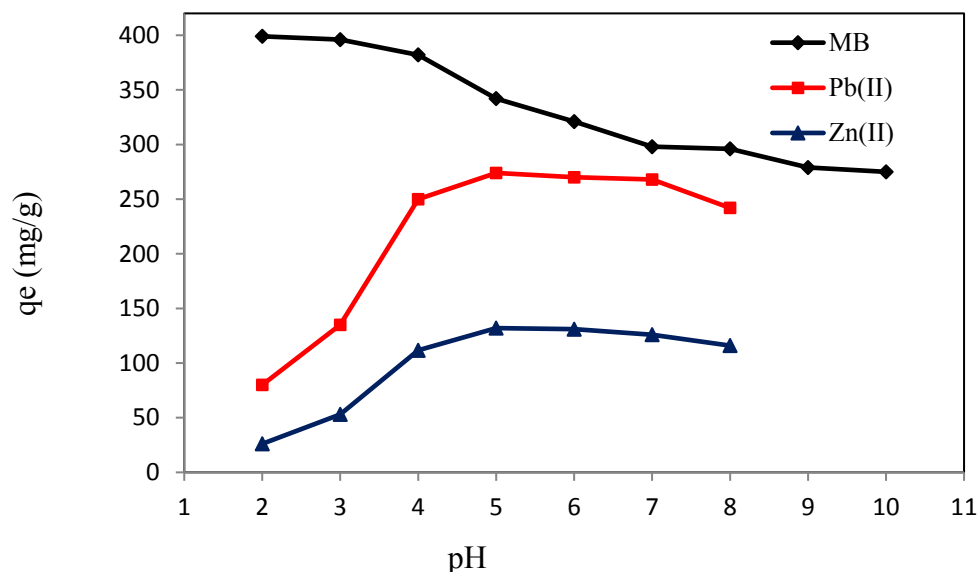

Figure 2. Effect of the pH of the solution on the adsorption of Pb (II), Zn (II), and MB by the synthesized nanocomposite (the initial concentration of 200 mg/L of the pollutant, the adsorbent dose of 0.5 g/L).

The ability of nanocomposite to adsorb MB at acidic pH values can be attributed to the electrostatic forces between the adsorbent and the MB anions. The positive charge of the surface at the pH values of lower than pH_{PZC} (due to the presence of H^+ and NH_3^+ belonging to chitosan) and the negative charge of methyl blue anions cause the formation of these electrostatic adsorption forces. While the same positive charge of the surface causes a repulsive force in confrontation with the metal cations. At the pH values of above pH_{PZC}, the nano sorbent surface is negatively charged and the electrostatic repulsion forces between the nano sorbent surface and the MB anions reduce the adsorption power.

3.3. Isotherms of the adsorption of the MB hydrocarbon anion by the EDTA/MnO₂/CS/Fe₃O₄ bio sorbent in the single-component adsorption

Adsorption isotherm experiments of Pb(II),

Zn(II), and MB by the EDTA/MnO₂/CS/Fe₃O₄ nanocomposite in a batch and single-component system were performed under the same conditions of the pH of 5, adsorbent dose of 0.5 g/L, temperature of 25 °C and time required to reach equilibrium. The purpose of these experiments was to find the maximum adsorption capacity and also to investigate the mechanism of the adsorption process using the values of the parameters of isothermal models. The equilibrium data of experiments related to each metal ion and MB were applied to estimate and evaluate the parameters of the models.

The results of the adsorption isotherm experiments and the isotherm models for Pb(II), Zn(II) were presented by the authors in another works [1]. The results of the isotherm model for the adsorption of MB on the nanocomposite have been presented in Figure 3.
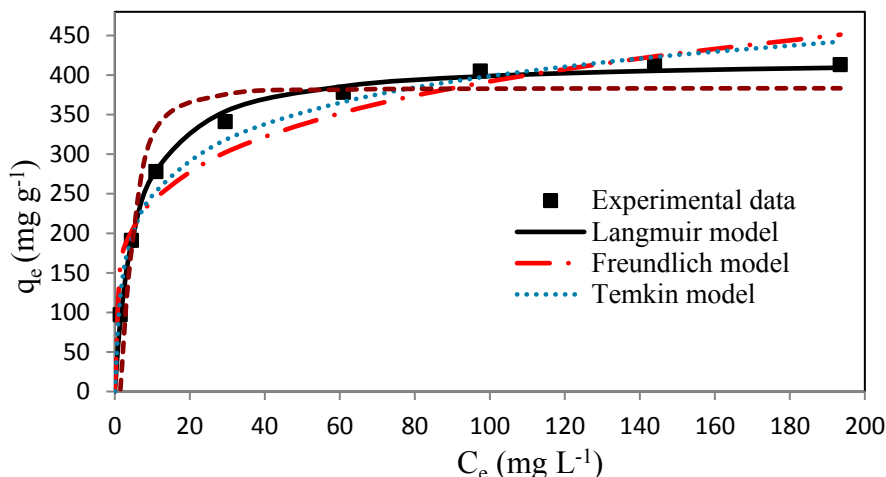
Figure 3. Adsorption isotherms of MB on the EDTA/γ-MnO$_2$/CS/Fe$_3$O$_4$ nanocomposite in a single component system (T= 25 °C, pH = 5, the absorbent dose = 0.5 g/L).

Results for the adsorption of the MB aromatic dye show that at low equilibrium concentrations (corresponding to low initial concentrations), the equilibrium adsorption capacity increases sharply by increasing the equilibrium concentration. This issue is owed to the presence of the active agents belonging to EDTA and chitosan, and unoccupied active sites related to γ-MnO$_2$ (to a greater extent) and Fe$_3$O$_4$ (to a lesser extent) on the nano sorbent surface. Further increasing of the equilibrium concentration of the contaminant causes the functional groups and active sites to become saturated, which result in vanishing the increasing trend of the equilibrium adsorption capacity in such a way that eventually remains constant at high equilibrium concentrations.

The values obtained for the parameters of the four isotherms using nonlinear regression analysis are presented in Table 6. According to the results, the Langmuir model which has the lowest error function values and the highest coefficients of R^2 is the most appropriate model for fitting the experimental data for the adsorption process of the considered metal cations and as well as MB aromatic dye.

Table 6
Parameters of the adsorption isotherms of Pb(II), Zn(II) [1], and MB in the separate adsorption system.

Isotherm	Parameter	Pb(II)	Zn(II)	MB
Langmuir model	q_m (mg/g)	310.4	136.0	421.1
	K_L (L/mg)	0.106	0.087	0.179
	R_L	0.045	0.067	0.014
	RMSE	7.263	1.800	6.722
	R^2	0.991	0.996	0.998
Freundlich model	K_F ((mg/g)(mg/L)$^{1/n}$)	74.42	31.58	147.03
	$1/n_F$	0.299	0.305	0.213
	RMSE	18.16	6.089	31.94
	R^2	0.942	0.950	0.950

Temkin model	b_T (kJ/mol)	0.044	0.092	0.038
	K_T	1.781	1.081	4.202
	RMSE	7.926	3.125	18.06
	R^2	0.988	0.987	0.985
Dobinin-Radushkevich model	q_{DR} (mg/g)	267.4	111.4	383.5
	B_{DR} (mol /J)$^2 \times 10^5$	0.90	0.497	0.306
	E (kJ/ mol)	0.237	0.317	0.403
	RMSE	24.19	11.45	43.86
	R^2	0.879	0.825	0.840

The compatibility of this model indicates that the EDTA/MnO$_2$/CS/Fe$_3$O$_4$ nanocomposite has a homogeneous surface with a uniform distribution of active sites. The maximum adsorption capacities calculated, using the Langmuir isotherm, for the adsorption of Pb(II), Zn(II), and MB in a single-component system are 310.4, 136.0 and 421.1 mg/g respectively. The values less than one for $1/n_f$ (from the dimensionless constants of the Freundlich model) indicate that the adsorption process is desirable for all three contaminants [31]. The values of b_T (related to adsorption heat) for the adsorption of Zn(II), Pb(II) and MB are 0.092, 0.044 and 0.038 kJ/mol respectively. Values less than 40 kJ/mol for this parameter reject the possibility of a chemical bond between the adsorbate and the nano sorbent surface. On the other hand, in the D-R model, the E values for both metal ions and MB are less than 8 kJ/mol, which confirm the physicality of the adsorption process of each of the contaminants [26, 32, 33].

3.4. Isotherms of the adsorption of Pb(II) metal cations and MB hydrocarbon anion by the EDTA/MnO₂/CS/Fe₄ nanocomposite in the two-component system

To investigate the simultaneous presence of two types of the contaminant in the solution,

adsorption experiments were performed in a two-component system. In these experiments, a constant initial concentration for one of the pollutants was used in all Erlenmeyer flasks, while the initial concentration of another pollutant varied from 25 to 300 mg/L in different Erlenmeyer flasks. After the adsorption by the nano sorbent (at the pH of 5 and adsorbent dose of 0.5 g/L) and reaching the equilibrium state in each of the laboratory containers, equilibrium concentrations were recorded, and the operation was repeated by changing the position of the two ions (in terms of the initial concentration value). The results of the adsorption in the two-component system of Pb(II) and Zn(II) metal cations were investigated and discussed in our other study [1]. In this work, the adsorption capacity of the nanocomposite for the simultaneous presence of Pb(II) as a metal cation and MB as an anion was studied. Figure 4a shows the effect of the simultaneous presence of Pb(II) and MB on the adsorption capacity of the nanocomposite in the adsorption of Pb(II). These results were obtained at a pH of 5 and an adsorbent dose of 0.5 g/L.

As observed, the presence of methyl blue reduces the adsorption capacity of the nanocomposite in the Pb(II) adsorption. Given the fact that methyl blue is an anion, it is expected that at the pH values of higher

than the pH$_{PZC}$ of the nanocomposite, the metal cation will prevail in the competition between the metal cation and the aromatic anion, but this does not occur due to the unique structure of methyl blue. Methyl blue has three groups of SO$_3^-$, which generate strong electrostatic attraction forces with the positive surface of the nanocomposite at acidic pH values. In addition to SO$_3^-$ groups, methyl blue has two -N = and one -NH- groups which are easily protonated and convert to NH$_3^+$. Therefore, methyl blue at the pH values of higher than pH$_{PZC}$ can also compete with metal cations and be adsorbed by the negatively charged surfaces. However, these electrostatic adsorption forces are much weaker than the adsorption forces created at acidic pH values. Figure 4b is related to the effect of the simultaneous presence of MB and Pb(II) on the adsorption capacity of the adsorbent in the MB adsorption. As observed, low initial concentrations of Pb(II) don't have great effects on the rate of the MB adsorption by the nanocomposite. This subject confirms the reasons mentioned for the effect of the presence of methyl blue on the adsorption capacity of the nanocomposite in the Pb(II) adsorption. The adsorption rate decreases at high concentrations of Pb(II) due to the reduction of the collision of methyl blue and adsorbent nanoparticles.
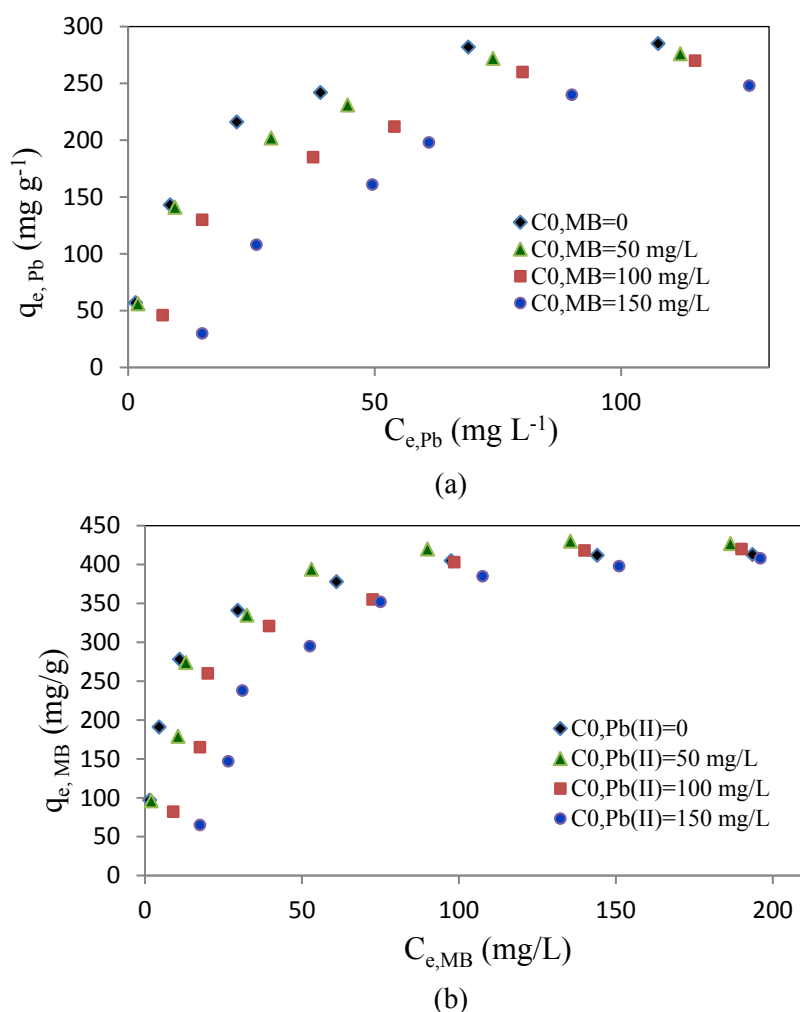

(a)

(b)

Figure 4. Effect of the simultaneous presence of Pb(II) and MB in the solution on the nano sorbent adsorption capacity in the adsorption of (a) Pb(II) and (b) MB (T= 25 °C, pH = 5, the absorbent dose = 0.5 g/L).

3.5. Nano sorbent recovery and reuse

The ability to recover and reuse nano sorbents is one of the basic criteria for selecting a nano sorbent, especially for industrial applications. In this research, for the recovery of the EDTA/γ-MnO$_2$/CS/Fe$_3$O$_4$ nanocomposite, initial (recovery) experiments were performed using several different acids including 0.1 M HCl and 0.1 M HNO$_3$ as the desorption agents of adsorbed contaminants. Considering the better performance of 0.1 M HCl, this acid was used in the adsorption-desorption cycles of the three studied contaminants in eight consecutive stages. Experimental parameters were selected according to the optimal conditions of the adsorption of target contaminants. Figure 5 shows the ratio of the nanocomposite adsorption capacity in each cycle to the initial adsorption capacity for all three contaminants.

As it can be seen, the adsorption capacity decreased with a moderate trend in the first five cycles for all three contaminants. In the fifth cycle, the capacity reduction compared to the first cycle is 3.6 %, 9.2 %, and 5.4 % for the adsorption of Pb(II), Zn(II) and MB respectively. In other words, in the case of Zn(II), the nanosorbent still has 90.8 % of the initial adsorption capacity for the adsorption of this ion. Therefore, it can be said that the understudy nanocomposite has a relatively good performance after five consecutive adsorption-desorption cycles. In subsequent cycles, a reduction in the adsorption capacity of the nanocomposite (especially in the Zn(II) adsorption) is observed. One of the reasons for the decrease in the adsorption capacity or efficiency of the nanosorbent is the change in the chemical nature of the nanosorbent surface and thus the reduction of the active functional groups on the surface following the continuous washing.
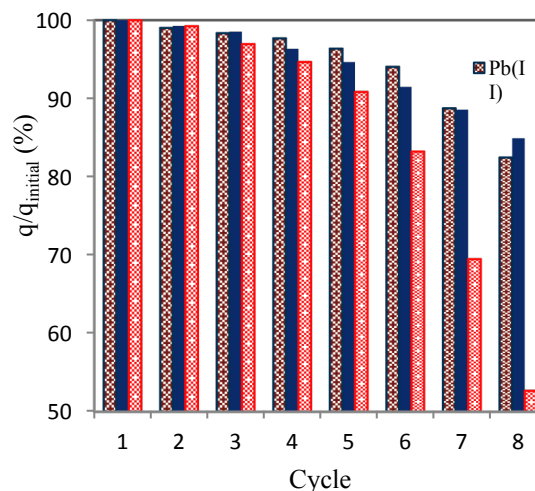

Figure 5. Ratio of the adsorption capacity in eight consecutive cycles of the nanocomposite recovery to the initial adsorption capacity.

4. Conclusions

The experimental design by RSM and the CCD method was used to find the optimal conditions for the adsorption of lead and zinc metal ions from the aqueous solution using the EDTA/γ-MnO$_2$/Chitosan/Fe$_3$O$_4$ multifunctional synthesized nanocomposite. The coefficients of the obtained statistical models showed that the initial concentration of metal ions has the greatest effect on the adsorption capacity. The highest removal predicted by the model for removing Pb(II) and Zn(II) from the aqueous solution were 100.776 % and 87.069 % respectively, that the value of more than 100 % for Pb(II) is due to the model's error. The optimal conditions for the mentioned responses for Pb(II) and Zn(II) were: the initial concentration of 34.379 and 29.285 mg/L, pH equal to 5.601 and 5.911, adsorbent dose of 0.892 and 0.877 g/L and contact time of 109.776 and 109.923 min respectively. The obtained actual experimental results were examined under the optimal conditions for Pb(II) and Zn(II) and had the maximum errors of 1.41 % and 2.2 % respectively. In the single-component

adsorption, the adsorption isotherms of Langmuir, Freundlich, Temkin, and Dubinin-Radushkovich were investigated. The results showed the dominance of the Langmuir isotherm in the adsorption of each of the three pollutants ($R^2 > 0.99$). The maximum adsorption rates according to the Langmuir model were 310.4 and 136 mg/g for lead and zinc ions respectively and 421.1 mg/g for methyl blue. The examination of the adsorption capacity after several consecutive cycles of the nanocomposite recovery showed that the studied nanocomposite at least has a high efficiency after five consecutive adsorption-desorption cycles.

References

[1] Panahandeh, A., Parvareh, A. and Keshavarz Moraveji, M., "Synthesis and characterization of γ-MnO$_2$/chitosan/Fe$_3$O$_4$ cross-linked with EDTA and the study of its efficiency for the elimination of zinc(II) and lead(II) from wastewater", *Environ. Sci. Pollut. Res.*, **28**, 9235 (2021).

[2] Wu, D., Wang, Y., Li, Y., Wei, Q., Hu, L., Yan, T., Feng, R., Yang, L. and Du, B., "Phosphorylated chitosan/CoFe$_2$O$_4$ composite for the efficient removal of Pb(II) and Cd(II) from aqueous solution: Adsorption performance and mechanism studies", *J. Mol. Liq.*, **277**, 181 (2019).

[3] Ali, H., Khan, E. and Ilahi, I., "Environmental chemistry and ecotoxicology of hazardous heavy metals: Environmental persistence, toxicity, and bioaccumulation", *J. Chem.*, Article ID 6730305, (2019).

[4] Feng, G., Ma, J., Zhang, X., Zhang, Q., Xiao, Y., Ma, Q. and Wang, S., "Magnetic natural composite Fe$_3$O$_4$-chitosan@bentonite for removal of heavy metals from acid mine drainage", *J. Colloid Interface Sci.*, **538**, 132 (2019).

[5] Dan, L., Liu, Y., Zhou, J., Yang, K., Lou, Z., Baig, S. A. and Xu, X., "Application of EDTA functionalized bamboo activated carbon (BAC) for Pb(II) and Cu(II) removal from aqueous solutions", *Appl. Surf. Sci.*, **428**, 648 (2018).

[6] Facchi, D. P, Cazetta, A. L., Canesin, E. A., Almeida, V. C., Bonafe, E. G., Kipper, M. J. and Martins, A. F., "New magnetic chitosan/alginate/ Fe$_3$O$_4$@SiO$_2$ hydrogel composites applied for removal of Pb(II) ions from aqueous systems", *Chem. Eng. J.*, **337**, 595 (2018).

[7] Depci, T., Kul, A. R. and Önal, Y., "Competitive adsorption of lead and zinc from aqueous solution on activated carbon prepared from Van apple pulp: Study in single- and multi-solute systems", *Chem. Eng. J.*, **200-202**, 224 (2012).

[8] Wang, H., Yuan, X., Wu, Y., Huang, H., Zeng, G., Liu, Y.,Wang, X., Lin, N. and Qi, Y., "Adsorption characteristics and behaviors of graphene oxide for Zn(II) removal from aqueous solution", *Appl. Surf. Sci.*, **279**, 432 (2013).

[9] Liu, C., Wu, T., Hsu, P. C., Xie, J., Zhao, J., Liu, K., Sun, J., Xu, J., Tang, J., Ye, Z., Lin, D. and Cui, Y., "Direct/alternating current electrochemical method for removing and recovering heavy metal from water using graphene oxide electrode", *ACS Nano*, **13**, 6431 (2019).

[10] Shabalala, A. N., Ekolu, S. O., Diop, S. and Solomon, F., "Pervious concrete reactive barrier for removal of heavy metals from acid mine drainage − Column study", *J. Hazard Mater.*, **323**, 641 (2017).

[11] Cui, L., Wang, Y., Gao, L., Hu, L., Yan, L., Wei, Q. and Du, B., "EDTA functionalized magnetic graphene oxide for removal of Pb(II), Hg(II) and Cu(II) in water treatment: Adsorption mechanism and separation property", *Chem. Eng. J.*, **281**, 1 (2015).

[12] Wu, D., Hu, L., Wang, Y., Wei, Q., Yan, L., Yan, T., Li, Y. and Du, B., "EDTA modified β cyclodextrin/chitosan for rapid removal of Pb(II) and acid red from aqueous solution", *J. Colloid Interface Sci.*, **523**, 56 (2018).

[13] Petrella, A., Spasiano, D., Acquafredda, P., De Vietro, N., Ranieri, E., Cosma, P., Rizzi, V., Petruzzelli, V. and Petruzzelli, D., "Heavy metals retention (Pb(II), Cd(II), Ni(II)) from single and multimetal solutions by natural biosorbents from the olive oil milling operations", *Process Saf. Environ.*, **114**, 79 (2018).

[14] Mousavi, S. J., Parvini, M. and Ghorbani, M., "Experimental design data for the zinc ions adsorption based on mesoporous modified chitosan using central composite design method", *Carbohydr. Polym.*, **188**, 197 (2018).

[15] Silva, S. B. D., Krolicka, M., Broek, L. A. M., Frissen, A. E. and Boeriu, C. G., "Water-soluble chitosan derivatives and pH-responsive hydrogels by selective C-6 oxidation mediated by TEMPO - laccase redox system", *Carbohydr. Polym.*, **186**, 299 (2018).

[16] Mallekpour, S. and Madani, M., "Functionalized-MnO_2/chitosan nanocomposites: A promising adsorbent for the removal of lead ions", *Carbohydr. Polym.*, **147**, 53 (2016).

[17] Kobylinska, N., Kostenko, L., Khainakov, S. and Garcia-Granda, S., "Advanced core-shell EDTA-functionalized magnetite nanoparticles for rapid and efficient magnetic solid phase extraction of heavy metals from water samples prior to the multi-element determination by ICP-OES", *Microchim. Acta.* **187** (5), 289 (2020).

[18] Ritonga, H., Nurfadillah, A., Rembon, F. S., Ramadhan, L. O. A. N. and Nurdin, M., "Preparation of chitosan-EDTA hydrogel as soil conditioner for soybean plant (Glycine max)", *Groundw. Sustain. Dev.*, **9**, 100277 (2019).

[19] Sabrina, F. L., Andrei, V. I., Luana, P., Guilherme, L. D., Luiz, A. A. P. and Tito, R. S. C., "Preparation of activated carbon from black wattle bark waste and its application for phenol adsorption", *J. Environ. Chem. Eng.*, **7** (5), 103396 (2019).

[20] Martín-Lara, M. A., Calero, M., Ronda, A., Iáñez-Rodríguez, I. and Escudero, C., "Adsorptive behavior of an activated carbon for bisphenol A removal in single and binary (bisphenol A—heavy metal) solutions", *Water*, **12** (8), 2150 (2020).

[21] Taoufik, N., Elmchaouri, A., Mahmoudi, S. A., Korili, S. A. and Gil, A., "Comparative analysis study by response surface methodology and artificial neural network on salicylic acid adsorption optimization using activated carbon", *Environ. Nanotechnol. Monit. Manag.*, **15**, 100448 (2021).

[22] Khanniri, E., Yousefi, M., Mortazavian, A. M., Khorshidian, N., Sohrabvandi, S., Arab, M. and Koushki, M. R., "Effective removal of lead (II) using chitosan and microbial adsorbents: Response surface methodology (RSM)", *Int. J. Biol. Macromol.*, **178**, 53 (2021).

[23] Sawood, G. M., Mishra, A. and Gupta, S.

K., "Optimization of arsenate adsorption over aluminum-impregnated tea waste biochar using RSM–central composite design and adsorption mechanism", *J. Hazard. Toxic Radioact. Waste*, **25** (2), 04020075 (2021).

[24] Cheraghipour, E. and Mahmoud Pakshir, M., "Environmentally friendly magnetic chitosan nano-biocomposite for Cu(II) ions adsorption and magnetic nano-fluid hyperthermia: CCD-RSM design", *J. Environ. Chem. Eng.*, **9** (2), 104883 (2021).

[25] Achour, Y., Bahsis, L., Ablouh, E. H., Yazid, H., Laamari, M. R. and Haddad, M., "Insight into adsorption mechanism of Congo red dye onto Bombax Buonopozense bark activated-carbon using central composite design and DFT studies", *Surf. Interfaces*, **23**, 100977 (2021).

[26] Alipour, M., Zarinabadi, S., Azimi, A. M. and Mirzaei, M., "Adsorptive removal of Pb(II) ions from aqueous solutions by thiourea- functionalized magnetic ZnO/nanocellulose composite: Optimization by response surface methodology (RSM)", *Int. J. Biol. Macromol.*, **151**, 124 (2020).

[27] Jafarnejad, M., Asli, M. D., Taromi, F. A. and Manoochehri, M., "Synthesis of multi-functionalized Fe_3O_4-NH_2-SH nanofiber based on chitosan for single and simultaneous adsorption of Pb(II) and Ni(II) from aqueous system", *Int. J. Biol. Macromol.*, **148**, 201 (2020).

[28] Biswas, S., Sen, T. K., Yeneneh, A. M. and Meikap, B. C., "Synthesis and characterization of a novel Ca-alginate-biochar composite as efficient zinc (Zn_2^+) adsorbent: Thermodynamics, process design, mass transfer and isotherm modeling", *Sep. Sci. Technol.*, **54**, 359 (2019).

[29] Chen, B., Zhao, H., Chen, S., Long, F., Huang, B., Yang, B. and Pan, X., "A magnetically recyclable chitosan composite adsorbent functionalized with EDTA for simultaneous capture of anionic dye and heavy metals in complex wastewater", *Chem. Eng. J.*, **356**, 69 (2019).

[30] Aghazadeh, M., Asadi, M., Maragheh, M. G., Ganjali, M. R., Norouzi, P. and Faridbod, F., "Facile preparation of MnO_2 nanorods and evaluation of their supercapacitive characteristics", *Appl. Surf. Sci.*, **364**, 726 (2015).

[31] Zeng, M., Zhang, X., Shao, L., Qi, C. and Zhang, X. M., "Highly porous chitosan microspheres supported palladium catalyst for coupling reactions in organic and aqueous solutions", *J. Organomet. Chem.*, **704**, 29 (2012).

[32] Dinh, V. P, Li, N. C., Tuyen, A., Hung, N. Q., Nguyen, V. D. and Nguyen, N. T., "Insight into adsorption mechanism of lead(II) from aqueous solution by chitosan loaded MnO_2 nanoparticles", *Mater. Chem. Phys.*, **207**, 294 (2018).

[33] Liu, Y., Xiong, Y., Xu, P., Pang, Y. and Du, C., "Enhancement of Pb (II) adsorption by boron doped ordered mesoporous carbon: Isotherm and kinetics modeling", *Sci. Total Environ.*, **708**, 134918 (2020).